Computing C-space Entropy for View Planning for a Generic Range Sensor Model

Pengpeng Wang (pwangf@cs.sfu.ca) Kamal Gupta (kamal@cs.sfu.ca)

Robotics Lab
School of Engineering Science
Simon Fraser University
Burnaby, BC, Canada, V5A 1S6

Abstract

We have recently introduced the concept of C-space entropy as a measure of knowledge of C-space for sensor-based path planning and exploration for general robot-sensor systems [1, 2, 3, 5]. The robot plans the next sensing action to maximally reduce the expected C-space entropy, also called the maximal expected entropy reduction, or MER criterion. The expected C-space entropy computation, however, made two idealized assumptions. The first was that the sensor field of view (FOV) is a point; and the second was that no *occlusion (or visibility) constraints* are taken into account, i.e., as if the obstacles are transparent. We extend the expected C-space entropy formulation where these two assumptions are relaxed, and consider a generic range sensor with non-zero volume FOV and occlusion constraints, thereby modelling a real range sensor. Planar simulations show that (i) MER criterion results in significantly more efficient exploration than the naive physical space based criterion (such as maximize the unknown physical space volume), (ii) the new formulation with non-zero volume FOV results in further improvement over the point FOV based MER formulation. Real experimental results with the SFU eye-in-hand system, a PUMA 560 equipped with a wrist mounted range scanner [4] will be reported in the final version of the paper.

1 Introduction

While most research in sensor-based path planning and exploration has concerned itself with mobile robots, our recent work has concentrated on general robot-sensor systems, where the sensor is mounted on a robot with non-trivial geometry and kinematics [1, 2, 3, 4, 5]. See also [6, 7, 8, 9, 10]. This class of robots is broad and includes robots ranging from a simple polygonal robot to articulated arms, mobile-manipulator systems, and humanoid robots [10]. The sensor is assumed to be an "eye" type sensor that is capable of providing distances from a given vantage point (actual implementation may be a laser range scanner, passive stereo vision, etc.). Figure 1 shows a simple example of such a robot-sensor system — an eye-in-hand system — an articulated arm with a wrist mounted range sensor. The robot must simultaneously plan paths and sense its environment for obstacles. Unlike for a simple mobile robot (often modelled as a point, see [11] for next best view planning for mobile robots), where the robot can move (path planning) and what it should sense (view planning), has a much more complex relationship here [4]. "Where to move" is best posed and answered in configuration space, the natural space for path planning. In [1, 2, 5], we showed that the view planning problem is appropriately posed in the configuration space of the robot — the next view should be planned to give maximum knowledge or information (whether a configuration is free or in collision with an obstacle) of the C-space of the robot. What this implies is that the sensing action, which obviously senses physical space, must be (implicitly or explicitly) transformed to the configuration space. Treating the unknown environment stochastically, we introduced the notion of C-space entropy as a measure of the robot's knowledge of C-space. The next best view is then the one that maximizes the expected entropy reduction (MER criterion) or, equivalently expected information gain. In contrast, earlier approaches had simply used a naive criterion, such as maximize unknown physical space volume (MPV) in the senor FOV, to choose the next best view [6].

In [1, 3] we derived closed form expressions for expected C-space entropy reduction, or information gain under a Poisson point process model of the environment [13]. However, two idealized assumptions were made regarding the sensor in that paper: (i) the sensor has a point field of view (FOV), i.e., it senses a single point and (ii) no occlusion constraints were taken into account, i.e., as if the sensor would "see" (get range measurement) through the obstacles. The

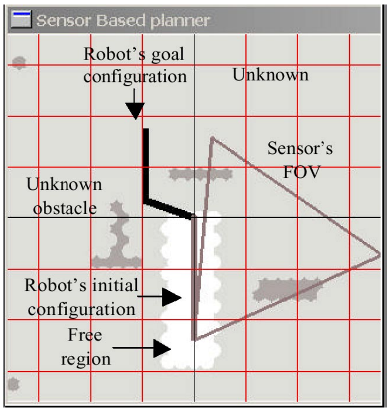

Figure 1: *An eye-in-hand system — a two-link robot with a wrist mounted range sensor (with triangle FOV) moving in an unknown environment. A key question (the view planning problem) is: where should the robot sense next?*

next best view is planned using this formulation, i.e., the algorithm computes the point (say, x_{max}) which, if sensed, would yield maximum expected information gain and places the sensor so that the center of the actual FOV (a cone) coincides with x_{max}. In [5], this formulation was extended for a beam sensor – the sensor FOV is a ray (beam) of finite length. In other words, assumption (ii) above was relaxed, but assumption (i), that sensor FOV has finite volume was still there. zero volume FOV while respecting occlusion constraints.

In this paper, we present the MER computation for a generic range sensor that has a non-zero volume FOV and its sensing action is subject to occlusion constraint, thereby modelling real range sensors. This computation is valid for a Poisson point process model of the environment, admittedly a simplification, but the resulting closed form expressions give us insights and are useful at least as approximations. We present simulations that show clear improvement in the efficiency of exploration with the new formulation. Our initial simulations are planar for ease of visualization. We emphasize that our formulations and results are valid for 3D environments and are currently being implemented on a real six-dof SFU eye-in-hand system consisting of a PUMA 560 with a wrist mounted area-scan laser range sensor that has been developed in our lab and was reported in [4]. We expect to report these experimental results in the final version of the paper.

2 Notation

Let $\mathcal{A}$ denote the robot and q denote a point in its configuration space, $\mathcal{C}$. $\mathcal{A}(q)$ then denotes the region in physical space, $\mathcal{P}$, occupied by the robot. Let $\mathcal{S}$ denote a sensor attached to the robot. We attach a coordinate frame to the sensor's origin. Let s denote the vector of parameters that completely determine the sensor frame, i.e., sensor's configuration. For instance, assuming the sensor is attached to the end-effector of the robot, for planar case, $s = (x, y, \theta)$; for 3D case, $s = (x, y, z, \alpha, \beta, \gamma)$. The sensor configuration space, denoted by $\mathcal{C}_s$, is the space of all possible sensor configurations. Let $\mathcal{V}(s) \in \mathcal{P}$ denote the region sensed (sensor FOV) by the sensor at configuration s. Subscripts $free$, obs, and unk (or sometimes u) denote the known free, known obstacle and unknown regions, respectively in physical and configuration space. So, for example $\mathcal{P}_{obs}$ denotes the known obstacles in physical space, $\mathcal{A}_{unk}(q)$ denotes the part of robot lying in unknown physical space at configuration q, and $\mathcal{C}_{free}$ denotes the known free configuration space.

3 Background: C-space Entropy and IGF

We assume that the obstacles' distribution in the physical environment is modelled with an underlying stochastic process (e.g., the Poisson model used later). The kinematics and geometry of the robot, embodied by function $\mathcal{A}(q)$ map the probability distribution in physical space to a probability distribution over the C-space. Shannon's Entropy then provides a measure of the robot's ignorance of the status of C-space. For a generic range sensor, which senses a region of non-zero volume, one can compute the expected entropy reduction if a sensing action, s, is taken, i.e., $\mathcal{V}(s)$ is sensed.

The information gain (IG) function captures this notion and is defined as

$$IG_{\mathcal{C}}(s) = -\underset{s}{E}\{\triangle H(\mathcal{C})\}$$

where $H(\mathcal{C})$ denotes the current C-space entropy, $\underset{s}{E}\{\triangle H(\mathcal{C})\} = E\{H(\mathcal{C} \mid \mathcal{V}(s)\} - H(\mathcal{C})$ denotes the expected entropy change after $\mathcal{V}(s)$, the region to sense at the sensor's configuration, s, is sensed.

In order to get efficiency in computing, we neglect the mutual entropy terms, essentially treating each robot's configuration as an independent random variable, i.e., $\widetilde{H}(\mathcal{C}) = \sum_{q \in \mathcal{C}} H(Q)$. In this equation, Q denotes the binary random variable (r.v.) corresponding to configuration q being free (=0) or in collision (=1); $H(Q)$ denotes the entropy of r.v. Q, i.e.,

$$H(Q) = p(q)\log(p(q)) + (1 - p(q))\log(1 - p(q)) \qquad (1)$$

where $p(q) = \Pr[q = free]$ is the marginal probability that configuration q is collision-free, also called the void probability of q. With this simplification one can show that:

$$\widetilde{IG}_{\mathcal{C}}(s) = -\underset{s}{E}\{\triangle \widetilde{H}(\mathcal{C})\} = \sum_{q \in \mathcal{C}} ig_q(s)$$

where $ig_q(s)$ is given by:

$$ig_q(s) = -\underset{s}{E}\{\triangle H(Q)\} \qquad (2)$$

When $\mathcal{V}(s)$ is sensed, the sensed information affects the C-space entropy via each robot's configuration q. $ig_q(s)$ is then the partial contribution to information gain via configuration q, if a region $\mathcal{V}(s)$ were to be sensed. Furthermore, $ig_q(x)$ equals 0 when

$\mathcal{A}(q)$ does not intersect $\mathcal{V}(s)$. So we need only compute the above summation over those q's such that $\mathcal{V}(s) \cap \mathcal{A}_{unk}(q) \neq 0$. Set of configurations q's such that $\mathcal{V}(s) \cap \mathcal{A}_{unk}(q) \neq 0$ is defined as the C-zone of s, denoted by $\chi(s)$. Therefore one can write:

$$IG_{\mathcal{C}}(s) = \sum_{q \in \chi(s)} ig_q(s)$$

4 Generic Sensor Model

We now consider a range sensor whose FOV has nonzero volume, i.e., $\mathcal{V}(s)$ is an open set in R^3 and the the actual volume sensed is governed by occlusion constraints. Most commercially available range sensors that provide range images (such as the area scan laser range sensors used in SFU eye-in-hand system [4]) fall into this category. Fig. 2 shows a schematic diagram as the sensor senses an unknown region within its FOV. As before, let $\mathcal{V}_u(s)$ denote the portion of the FOV that intersects $\mathcal{P}_u$ and is not occluded by known obstacles. Note that $\mathcal{V}_u(s)$ might be a multiply-connected set. In the figure, $\mathcal{V}_u(s)$ consists of regions A, B, C and D (region E is excluded from $\mathcal{V}_u(s)$ since it is occluded by a known obstacle. After sensing, regions A, B and C become free; region D remains unknown because it is occluded by the sensed obstacles (shown in dark). Of course, the sensor also provides the distances from the sensor's origin to the sensed obstacles.

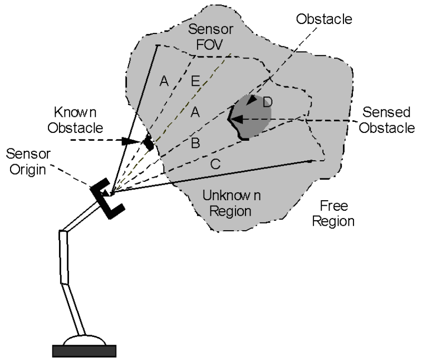

Figure 2: *Illustration of a generic range sensor's FOV $\mathcal{V}(s)$. After this sensing action, regions A, B and C become free, the black contour is a sensed obstacle and region D, occluded by the sensed obstacle remains unknown. Region E also remains unknown, but it is occluded by an already known obstacle.*

4.1 Environmental Model

Again, we are using Poisson point process to make a simple model of the robot's workspace. Poisson point process is essentially characterized by uniformly distributed points in space [13]. In robot motion planning context, these points, denoted by pt, are obstacles. Given the density parameter of this model, λ, the void probability of an arbitrary set $\mathcal{B} \in \mathcal{P}$ — the probability that there is no point (obstacle) in $\mathcal{B}$ — denoted by $p(\mathcal{B})$, is given by

$$p(\mathcal{B}) = \Pr[no\ pt\ \in \mathcal{B}] = e^{-\lambda \cdot vol(\mathcal{B})} \tag{3}$$

This implies that $p(q)$, the void probability of a robot configuration q is given by

$$p(q) = \Pr[no\ pt\ \in \mathcal{A}(q)] = e^{-\lambda \cdot vol(\mathcal{A}_{unk}(q))} \tag{4}$$

Because the sensing is subject to occlusion constraint, the sensor can only detect the very first point obstacle along each sensing ray. This very first ostacle is called the hit point and is denoted by *hitpt*, . The sensing action can therefore be easily visualized as finding a bunch of new hit-points' positions in the workspace.

4.2 $ig_q(s)$ Computation

For a given q, $ig_q(s)$ is composed of sum of two components, i.e., $ig_q = (ig_q)_1 + (ig_q)_2$. The first component, $(ig_q)_1$, corresponds to those outcomes where the sensor would sense at least one hit point inside $\mathcal{A}(q) \cap \mathcal{V}_u(s)$, i.e., $hitpt \in \mathcal{A}(q) \cap \mathcal{V}_u(s)$. Let this set of outcomes be denoted event 1. After sensing, the robot, were it to be placed at configuration q, $\mathcal{A}(q)$, would be in collision with an obstacle (the sensed hit point). So $H(Q \mid \text{event } 1) = 0$ and $\underset{event\ 1}{\triangle} H(Q) = H(Q \mid \text{event } 1) - H(Q) = -H(Q)$.
It turns out (not unexpectedly in the light of our earlier beam sensor result reported in [5], however several technical details need to be carefully worked out) that the probability of event 1, $\Pr[\exists hitpt \in \mathcal{A}(q) \cap \mathcal{V}_u(s)]$, is the same as $\Pr[\exists pt \in \mathcal{A}(q) \cap \mathcal{V}_u(s)]$, as if occlusion does not matter! Theorem 2 states this result formally. But first we show an intermediate result, that the probability of all the point obstacles inside $\mathcal{B}$ to be occluded by point obstacles in front of them is zero!

Theorem 1. $\Pr[all\ pts \in \mathcal{B}\ are\ occluded] = 0$ *where* $\mathcal{B} \subseteq \mathcal{V}_u(s)$ *is any open set and pt are point obstacles whose distribution is governed by a Poisson point process.*

Proof. We first discretize $\mathcal{V}_u(s)$ into M number of nearly-identical cones, $\mathcal{V}_1, \mathcal{V}_2, \ldots, \mathcal{V}_M$ as shown in Fig. 3. Consider a cone (with apex at sensor origin) which contains $\mathcal{V}(s)$. Lay a discrete grid of size ϵ and connect the boundary of these cells to the sensor's origin. $\mathcal{V}_u(s)$'s functionality can then be captured by these cones. As M approaches infinity, the discrete model approaches the continuous model.

Note that $\mathcal{B}$ is also discretized by these $\mathcal{V}_i$'s. We label those discretized cones that have common part with $\mathcal{B}$ by $\mathcal{VB}_1, \mathcal{VB}_2, \ldots, \mathcal{VB}_{M'}$. We denote the intersection of these $\mathcal{VB}_i$'s with every component of $\mathcal{B}$ by $\mathcal{B}_1, \mathcal{B}_2, \ldots, \mathcal{B}_{M''}$ respectively and use $front(B)_i$ to denote the subset of $\mathcal{VB}_i \setminus \mathcal{B}$, ("$\setminus$" here denotes the set minus operation), that is in front of $\mathcal{B}_i$ along the sensing direction.[1]

We know that the set of outcomes denoted by $Event(all\ pts \in \mathcal{B}\ are\ occluded)$ is a subset of outcomes denoted by $Event(\exists occluded\ pt \in \mathcal{B})$, i.e., at least one point, pt, inside $\mathcal{B}$ is occluded. Hence, we have $\Pr[all\ pts \in \mathcal{B}\ are\ occluded] \leq$

[1] Note that $\mathcal{B}$ could be a multiple-connected set. So the number of $\mathcal{B}_i$'s, M'' could be greater than the number of discretized cones, M. And since the labelling sequence is irrelevant to our proof, we can arbitrarily label these $\mathcal{B}_i$'s

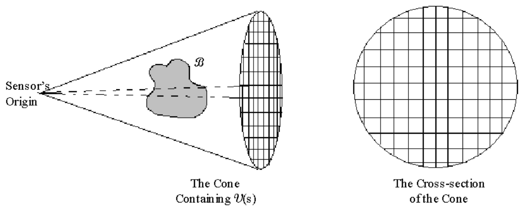

Figure 3: *Illustration of a possible way of discretizing* $\mathcal{V}_u(s)$.

$\Pr[\exists occluded\ pt \in \mathcal{B}]$. Furthermore, since $Event(all\ pts \in \mathcal{B}\ are\ occluded)$ implies that at least one point is inside the region $\mathcal{B}_i$, and at least one point is inside $front(B)_i$. So we have

$$\begin{aligned}
&\Pr[\exists occluded\ pt \in \mathcal{B}]\\
= &\sum_{i=1}^{M''}(\Pr[\exists pt \in \mathcal{B}_i]\cdot\Pr[\exists pt \in front(B)_i])\\
- &\sum_{i=1}^{M''}\sum_{\substack{j'\neq i\wedge\mathcal{B}_i\mathcal{B}_{j'}\notin\\ the\ same\ cone}}^{M''}(\Pr[\exists pt \in \mathcal{B}_i]\cdot\Pr[\exists pt \in front(B)_i]\\
\cdot\ &\Pr[\exists pt \in \mathcal{B}_{j'}]\cdot\Pr[\exists pt \in front(B)_{j'}])+\ldots\\
\leq &\sum_{i=1}^{M''}\Pr[\exists pt \in \mathcal{B}_i]\cdot\Pr[\exists pt \in front(B)_i]
\end{aligned}$$

The reason for inequality sign above is as follows. We regard $Event(\exists occluded\ pt \in \mathcal{B})$ as the summation of the events that occlusion happens in any of the $\mathcal{B}_i$'s (the expression on the right side of inequality sign) minus the "double counting" that occurs. This "double counting" is essentially the probability of the joint event that occlusion happens concurrently in more than one $\mathcal{B}_i$'s and hence it is always greater than or equal to zero, and hence the inequality sign.[2]

In the above summation, for the term $\Pr[\exists pt \in front(B)_i]$, using Eq. (3), we have $\Pr[\exists pt \in front(B)_i] = 1-e^{-\lambda\cdot vol(front(B)_i)}$. Since the volume of $front(B)_i$ is less than or equal to the volume of the biggest discretized cone, denoted by $\mathcal{VB}_{max}$, we will have $\Pr[\exists pt \in front(B)_i] \leq 1-e^{-\lambda\cdot vol(\mathcal{VB}_{max})}$.

Now substituting the term $\Pr[\exists pt \in front(B)_i]$ by $1-e^{-\lambda\cdot vol(\mathcal{VB}_{max})}$ and taking it out of the summation, we have,

$$\Pr[\exists occluded\ pt \in \mathcal{B}] \leq (1-e^{-\lambda\cdot vol(\mathcal{VB}_{max})})\cdot\sum_{i=1}^{M'}\Pr[\exists pt \in \mathcal{B}_i]$$

For the term $\Pr[\exists pt \in \mathcal{B}_i]$, using Eq. (3) with only first order expansion, we have,

$$\Pr[\exists pt \in \mathcal{B}_i] = 1-e^{-\lambda\cdot vol(\mathcal{B}_i)} = \lambda\cdot vol(\mathcal{B}_i)$$

This approximation is reasonable since the volume, $vol(\mathcal{B}_i)$, is small enough when the discretization resolution is small enough.

Therefore, we have,

$$\begin{aligned}
&\Pr[all\ pts \in \mathcal{B}\ are\ occluded] \leq \Pr[\exists occluded\ pt \in \mathcal{B}]\\
&\leq (1-e^{-\lambda\cdot vol(\mathcal{VB}_{max})})\cdot\sum_{i=1}^{M'}vol(\mathcal{B}_i)\cdot\lambda\\
&= (1-e^{-\lambda\cdot vol(\mathcal{VB}_{max})})\cdot vol(\mathcal{B}\cap\mathcal{V}_u(s))\cdot\lambda
\end{aligned}$$

As M approaches infinity, $vol(\mathcal{VB}_{max})$ approaches zero and therefore $(1-e^{-\lambda\cdot vol(\mathcal{VB}_{max})})$ approaches zero. So $\Pr[\exists occluded\ pt \in \mathcal{B}] = 0$, which implies $\Pr[all\ pts \in \mathcal{B}\ are\ occluded] = 0$. ∎

Theorem 2. $\Pr[\exists hitpt{\in}\mathcal{B}]{=}\Pr[\exists pt \in \mathcal{B}]{=}\ 1-e^{-\lambda\cdot vol(\mathcal{B})}$

Proof. The computation of $\Pr[\exists hitpt \in \mathcal{B}]$ is based on the complement of this event, $Event(no\ hitpt \in \mathcal{B})$, i.e., $\Pr[\exists hitpt \in \mathcal{B}] = 1-\Pr[no\ hitpt \in \mathcal{B}]$.

$Event(no\ hitpt \in \mathcal{B})$ can be divided into two events, the event that there are no point obstacles in $\mathcal{B}$ and the event that all the point obstacles inside $\mathcal{B}$ are occluded, $Event(all\ pts \in \mathcal{B}\ are\ occluded)$.

Using Eq.(3), the probability of $Event(no\ hitpt \in \mathcal{B})$ will be,

$$\Pr[no\ hitpt \in \mathcal{B}] = p(\mathcal{B}) + \Pr[all\ pts \in \mathcal{B}\ areoccluded]$$

Using Theorem 1, the second term is zero, and hence we have, $\Pr[no\ hitpt \in \mathcal{B}] = p(\mathcal{B})$. It then follows that the probability of the complement event, i.e., $\Pr[\exists hitpt \in \mathcal{B}] = 1-p(\mathcal{B}) = 1-e^{-\lambda\cdot vol(\mathcal{B})}$. ∎

So we have

$$\begin{aligned}
(ig_q)_1 &= \Pr[hitpt \in \mathcal{A}(q)\cap\mathcal{V}_u(s)]\cdot H(Q)\\
&= \Pr[pt \in \mathcal{A}(q)\cap\mathcal{V}_u(s)]\cdot H(Q)\\
&= (1-e^{-\lambda\cdot vol(\mathcal{A}(q)\cap\mathcal{V}_u(s))})\cdot H(Q) \qquad (5)
\end{aligned}$$

The second component, denoted by $(ig_q)_2$, corresponds to a set of outcomes in which there does not exist any hit-point inside $\mathcal{A}(q)\cap\mathcal{V}_u(s)$. In this case, the status of $\mathcal{A}(q)$ would either remain unknown, albeit the unknown portion (volume) may have decreased, or it may become completely free; but it will not be known to be in collision. Let us denote this set of outcomes by event 2. Using the discretized FOV as in Figure 3, let us denote the state of $A(q)\cap\mathcal{V}_u(s)$ after sensing by $\underline{J}$. Event 2 then corresponds to the set of outcomes $\{\underline{J}:\ \text{no}\ hitpt \in \mathcal{A}(q)\cap\mathcal{V}_u(s)\}$. By definition, then we have

$$(ig_q)_2 = \sum_{\underline{J}\in\text{event 2}}\Pr[\underline{J}]\cdot(H(Q)-H(Q\mid\underline{J})) \qquad (6)$$

where $\Pr[\underline{J}]$ is the probability of $\mathcal{A}(q)\cap\mathcal{V}_u(s)$ being in state $\underline{J}$ after sensing.

We show that the above expectation turns out to be that of the event (let us call it event 3) that there does not exist any pt in $\mathcal{A}(q)\cap\mathcal{V}_u(s)$, or equivalently that the region $\mathcal{A}(q)\cap\mathcal{V}_u(s)$ is free! This implies that occlusion does not matter in the expectation computation! It is not entirely unexpected in the light of beam sensor result, [5], however several technical details need to be worked out. Theorem 3 states this result formally.

Theorem 3.

$$\begin{aligned}
&\sum_{\underline{J}\in event\ 2}\Pr[\underline{J}]\cdot H(Q\mid\underline{J}) = \Pr[event\ 3]\cdot H(Q\mid event\ 3)\\
= \ &e^{-\lambda\cdot vol(\mathcal{A}(q)\cap\mathcal{V}_u(s))}\cdot H(Q\mid event\ 3) \qquad (7)
\end{aligned}$$

[2] This is nothing but a generalization of $p(A)+p(B)\geq p(A,B)$, where A and B are two random variables, and $p()$ denotes the probability.

Proof. Omitted for lack of space. ∎

Thus, expanding the summation in Eq. 6, we have,

$$(ig_q)_2 = H(Q) \cdot \sum_{\underline{J} \in \text{event } 2} \Pr[\underline{J}] - \sum_{\underline{J} \in \text{event } 2} \Pr[\underline{J}] \cdot H(Q \mid \underline{J}) \quad (8)$$

The first term (the first summation) above is $1 - \Pr[hitpt \in \mathcal{A}(q) \cap \mathcal{V}_u(s)]$. The expression for it is given by Theorem 2 if we substitute $\mathcal{A}(q) \cap \mathcal{V}_u(s)$ for $\mathcal{B}$. Furthermore, substituting from Theorem 3 for the second term, we get

$$\begin{aligned}(ig_q)_2 &= H(Q) \cdot \Pr[\text{event } 3] - \Pr[\text{event } 3] \cdot H(Q \mid \text{event } 3) \\ &= e^{-\lambda \cdot vol(\mathcal{A}(q) \cap \mathcal{V}_u(s))} \cdot (H(Q) - H(Q \mid \text{event } 3)) \quad (9)\end{aligned}$$

So summing the two components together, and using Eq. (5) and (9), we have

$$\begin{aligned}ig_q &= (ig_q)_1 + (ig_q)_2 \\ &= H(Q) - e^{-\lambda \cdot vol(\mathcal{A}(q) \cap \mathcal{V}_u(s))} \cdot H(Q \mid \text{event } 3) \quad (10)\end{aligned}$$

Both $H(Q \mid \text{event } 3)$ and $H(Q)$ in the above equation are determined using Eq. (1) and that $p(q \mid \text{event } 3) = e^{-\lambda \cdot vol(\mathcal{A}_u(q) \setminus \mathcal{V}_u(s))}$.

Note that this result reduces to the point FOV sensor model [1], and to the beam FOV sensor model [5], in the limit. The reduction can be shown in a straightforward manner and is omitted for brevity.

5 Algorithm for View Planning

Now that we have computed an expression for IG over sensor's configuration space, we can use the MER criterion to decide the next scan, i.e., choose the sensor configuration s_{max} such that $s_{max} = \max_s \{ \sum_{q \in \mathcal{X}_u(s)} ig_q(s) \}$. The algorithm then is as follows:

for every s /* *according to a certain resolution* */
  determine $\mathcal{V}_u(s)$
  $\widetilde{IG}(s) = 0$ /* *initialize* */
  for every q
    if ($\mathcal{A}_u(q)$ *overlaps with* $\mathcal{V}_u(s)$)
      compute $ig_q(s)$
    $\widetilde{IG}(s) = \widetilde{IG}(s) + ig_q(s)$
$s_{max} = \max_s(\widetilde{IG}(s))$

Determining $\mathcal{V}_u(s)$ corresponds to determining the intersection of the sensor FOV with $\mathcal{P}_u$ while excluding portions of $\mathcal{P}_u$ occluded by already known obstacles (before sensing action), a simple geometric computation. Note that iteration over q (C-space of the robot) may be prohibitive for robots with many degree of freedoms. In this case, the summation can be carried out over a large enough set of random samples.

6 Simulation Results

In order to test the effectiveness of our formulae, we conducted a series of experiments on the simulated two-link eye-in-hand preliminary system shown in Figure 1. The task for the robot is to explore its environment, strting from its initial configuration. The overall planner used is SBIC-PRM (sensor-based incremental construction of probabilistic road map) reported in [3, 4]. Briefly, SBIC-PRM consists of an incrementalized model-based PRM [14], that operates in the currently known environment; and a view planner that decides a reachable configuration within the currently known environment from which to take the next view, chosen according to a criteron. The two sub-planners operate in an interleaved manner.

We compare the results of four different view planning criteria for efficiency of exploration of the physical and configuration space. The first strategy, denoted by RV (random views), is to randomly choose a viewpoint as the next scan. The second, denoted by MPV (maximum unknown physical volume) is to choose the next viewpoint so as to maximize the unknown physical volume inside the scan [6]. The third is to use point FOV based MER criterion for view-planning [1, 2], and place the centre of the actual FOV (the cone) at x_{max}, the single point that results in maximum entropy reduction. The fourth is to use the generic non-zero volume FOV based MER criterion derived in this paper. In all these cases, the robot started off as in Figure 1.

As shown in the Figures 4, 5, 6, and 7, the first two strategies expand the known C-space much less than the last two MER criterion based strategy. Using RV gives us about 8% expansion of known C-space in 5 scans, and the robot reached its goal in 36 scans. MPV results in C-space expansion by about 54% in 5 scans. The point FOV based MER criterion gives much better results, resulting in about 73% expansion in 5 scans. The general FOV based MER criterion is the best, better than point FOV based MER. It made the C-space expand by about 82 % in 5 scans. For reader's information, although not relevant here, black dots in these figures are the nodes of the probabilistic roadmap used for planning paths.

Figure 8 plots C-space vs. number of iterations for the above four view-planning criteria. We can easily see that the generic range sensor based MER is the most efficient one, which expanded C-space to about 90% in 7 scans; point FOV based MER needed 11 scans; MPV needed 19 scans; and RV needed 33 scans.

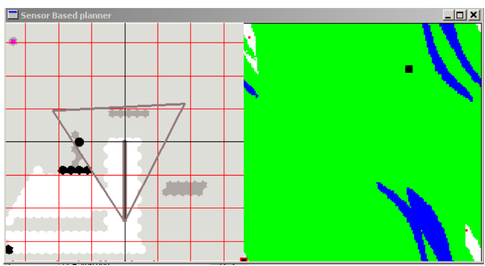

Figure 4: *Known Physical and C-space after 5 scans: RV criterion*

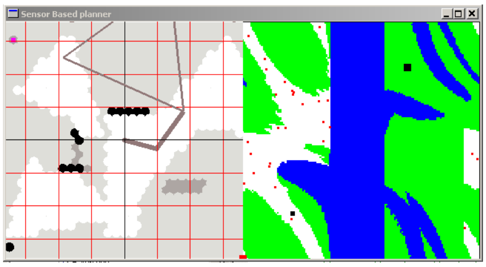

Figure 5: *Known Physical and C-space after 5 scans: MPV criterion*

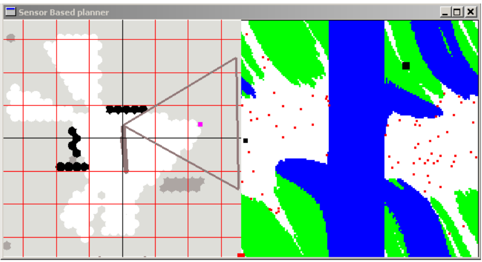

Figure 6: *Known Physical and C-space after 5 scans: Point FOV based MER criterion*

7 Conclusions

We presented closed form solutions for computing the expected C-space entropy reduction for a general non-zero volume FOV range sensor extending our previous results that applied to a point FOV sensor and take into account the occlusion constraints inherent in range sensors. Planar simulations show that our new results lead to more efficient exploration of the robot configuration space. Our next step is to implement these results for a real six-dof eye-in-hand system, a PUMA 560 with a wrist mounted area scan laser range finder.

The current formulation assumes a Poisson point process for obstacle distribution. It treats obstacles as points. Extending our formulation for a Boolean stochastic model [13] where geometric shape of obstacles is taken into account would be the next step.

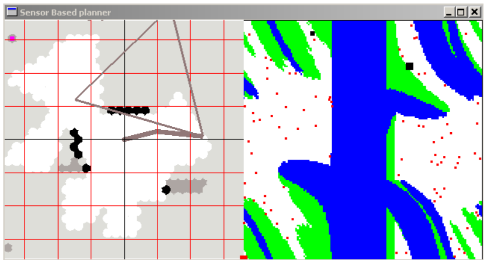

Figure 7: *Known Physical and C-space after 5 scans: Generic non-zero volume FOV based MER criterion.*

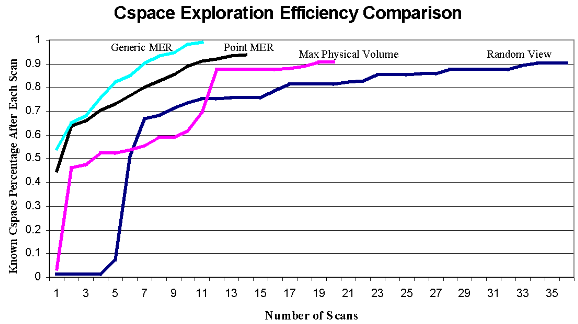

Figure 8: *The comparison of C-space exploration efficiency for the four view-planning algorithms: RV, MPV, Point FOV Based MER and Generic FOV Based MER*

References

[1] Y. Yu and K. Gupta, "An Information Theoretic Approach to View Planning with Kinematic and Geometric Constraints", Proc. IEEE ICRA, Seoul, Korea, May 21-26, 2001, pp. 1948-1953.

[2] Y. Yu, "An Information Theoretical Incremental Approach to Sensor-based Motion Planning for Eye-in-Hand Systems ", Ph.D. Thesis, School of Engineering Science, Simon Fraser University, 2000.

[3] Y. Yu and K. Gupta, "View Planning via C-Space Entropy for Efficient Exploration with Eye-in-hand Systems", Proc. VII Int. Symp. on Experimental Robotics, 2000. Available as lecture notes in Control and Information Sciences, LNCIS271, Springer. pp. 373-384.

[4] Y. Yu and K. Gupta, "Sensor-based Probabilistic Roadmaps: Experiments with an Eye-in-hand System", Advance Robotics, Vol.14, No.6, pp.515-537, 2000.

[5] P. Wang and K. Gupta, "Computing C-space Entropy for View Planning Based on Beam Sensor Model", To appear in Proc. Of IROS 2002.

[6] E. Kruse,R. Gutsche and F. Wahl,"Effective Iterative Sensor Based 3-D map Building using Rating Functions in Configuration Space", Proc. IEEE ICRA, 1996, pp.1067-1072.

[7] P. Renton, M. Greenspan, H. Elmaraghy, and H. Zghal, "Plan-n-Scan: A Robotic System for Collision Free Autonomous Exploration and Workspace Mapping", Jrnl. on Intell. And Robotic Systems, 24:207-234, 1999.

[8] J. Ahuactzin and A. Portilla, "A Basic Algorithm and Data Structure for Sensor-based Path Planning in Unknown Environment", Proc. Of IROS 2000.

[9] E. Cheung and V. J. Lumelsky, "Motion Planning for Robot Arm manipulators with Proximity Sensors", Proc. IEEE ICRA, Philadelphia, PA, 1988.

[10] H. Choset and J. W. Burdick, "Sensor based Planning for a Planar Rod Robot", Proc. of the IEEE ICRA, Minneapolis, MN, 1996.

[11] H. G. Banos and J. C. Latombe, "Robot Navigation for Automatic Construction Using Safe Regions", Preprints Proc. ISER 2000, pp. 395-404.

[12] K. Hirai, M. Hirose, M. Haikawa and T. Takenaka, "The Development of HONDA Humanoid Robot", Proc. Of ICRA 1998, pp. 1321-1326.

[13] D. Stoyan and W.S. Kendall, Stochastic Geometry and Its Applications, J. Wiley, 1995.

[14] L. Kavraki, P. Svestka, J. Latombe and M. Overmars, Probabilistic Roadmaps for Path Planning in High-dimensional Configuration Spaces, IEEE Transactions on Robotics and Automation, 12(4): 556-580, Aug. 1996.